

Mapping of mutation-sensitive sites in protein-like chains.

M. Skorobogatiy^{1*} and G. Tiana^{2,3}

¹ *Department of Physics, MIT, Cambridge, USA*

² *Department of Physics, DTU, building 307, 2100 Lyngby, Denmark*

³ *Dipartimento di Fisica, Università di Milano, Via Celoria 16, I-20133 Milano, Italy*

(August 22, 2018)

Pacs numbers: 87.15.Da, 61.43.-j, 64.60.Cn, 64.60.Kw

Abstract

In this work we have studied, with the help of a simple on-lattice model, the distribution pattern of sites sensitive to point mutations ('hot' sites) in protein-like chains. It has been found that this pattern depends on the regularity of the matrix that rules the interaction between different kinds of residues. If the interaction matrix is dominated by the hydrophobic effect (Miyazawa Jernigan like matrix), this distribution is very simple - all the 'hot' sites can be found at the positions with maximum number of closest nearest neighbors (bulk).

If random or nonlinear corrections are added to such an interaction matrix the distribution pattern changes. The rising of collective effects allows the 'hot' sites to be found in places with smaller number of nearest neighbors (surface) while the general trend of the 'hot' sites to fall into a bulk part of a conformation still holds.

I. INTRODUCTION

In this paper we study how the choice of a particular Hamiltonian is responsible for the distribution pattern of sites sensitive to point mutations in a Heteropolymeric chain.

As shown in [1] using a very simple model [2], in every optimized [3] sequence there are sites at which point mutations are likely to cause misfolding of the native state (we call them 'hot' sites), while there are other sites at which point mutations have no relevant thermodynamic effect ('cold' sites), and we call intermediate sites 'warm'. As known from both experimental [4] and theoretical studies [1] usually proteins are made of few 'hot' sites while the majority of the other sites are 'cold'. Because of the thermodynamic importance of the 'hot' sites it is of general interest to investigate the principles guiding their positioning along the protein chain.

The model used in this work describes the polymer as a chain of beads in a cubic lattice, interacting through the Hamiltonian

$$H = \frac{1}{2} \sum_{ij}^L B_{ij} \Delta(r_i - r_j), \quad (1)$$

where B_{ij} is the contact energy between the two residues situated on the i -th and j -th positions, L is the length of the chain and $\Delta(r_i - r_j)$ has the value 1 if the i -th and j -th are nearest neighbors and zero if not.

In literature, different choices of the matrix B_{ij} have been used. The results of Ref. [1,2] have been found with a matrix [5] whose elements are distributed according to a Gaussian, with average $\overline{B} = 0$ and standard deviation $\sigma = 0.3$ (in units of $kT = 0.6 \text{ kcal/mol}$). With these matrix elements, for every target structure it is possible to select sequences whose native state is unique, stable and kinetically accessible [6]. It has been found that a reliable condition for a site to be 'cold' or 'hot' is intimately connected to the change in the native state energy caused by a point mutation: the bigger is this difference, the more probable for this site to be a 'hot' site. Hot sites of such sequences are mainly in the bulk sites of the native conformation, but can be on the surface as well, while some bulk sites can be rather insensitive to mutations (Fig.1a).

Repeating the same calculations with a random-generated, Gaussian-distributed set of interaction energies, we have observed similar distribution patterns for 'hot' and 'cold' sites (Fig.1b).

Another choice of the interaction matrix can be made to take into account explicitly the hydrophobic effect encountered in real proteins. The simplest way is to choose the matrix B_{ij} to be composed of only three different elements, namely B_{HH} , B_{PP} and $B_{HP} = B_{PH}$, where $B_{HH} < B_{PP} < B_{HP}$. These elements are responsible for the interaction between hydrophobic (H) and polar (P) residues. Unfortunately it was found [2] that for a given target structure and 'HP' interaction matrix it is difficult to construct optimal sequences for which this target structure would be kinetically accessible. As a rule, the optimization of the sequence puts H-residues in the bulk sites (the sites with the greatest number of nearest-neighbors), and every substitution of an H residue with a P residue causes the chain misfolding (See Figs. 2 and 3 in Ref. [7]).

On the way between the random matrix and the highly regular HP interaction model stands the matrix deduced by Miyazawa and Jernigan in [8]. This matrix contains 210 different elements which can still be grouped into 3 big blocks, according to their hydrophobicity. In this case it is possible to find sequences for which the native state is both stable and kinetically accessible. It was also found that, as in the situation with only two kinds of residues, 'hot' sites are invariably the sites with the highest number of contacts (bulk sites, Fig. 1d).

The question again is what are the principles guiding the positioning of 'hot' sites along the protein chain and how a particular form of the interaction matrix can influence the distribution pattern of 'hot' and 'cold' mutation sites. This paper is organized as following. In the next section we will present a convenient representation of an interaction matrix as a function of 'mixing' parameter β . Variation of the 'mixing' parameter will correspond to a change from highly ordered HP like interaction matrix at $\beta = 0$ to highly nonlinear matrix at non-zero values of 'mixing' parameter. A distribution pattern of 'cold' and 'hot' sites will be investigated with the use of these interaction matrices. Next we will address the same

question by introducing a parameter of 'randomness' γ which would allow us to investigate the mutation sites distribution pattern with highly ordered HP like interaction matrix at $\gamma = 0$ and random Gaussian interaction matrix at large γ . Conclusions will be drawn at the end.

II. LTW PARAMETERIZATION

In the work by Lee, Tang and Wingreen [9] a particular interesting parameterization of semi-experimental MJ matrix [8] was introduced, as a consequence of its regularity. In their work it was shown that elements of the MJ interaction matrix can be very nicely fitted as

$$B_{\alpha\gamma} = q_{\alpha} + q_{\gamma} + \beta q_{\alpha} q_{\gamma}, \quad (2)$$

where q_{α} is ascribed to a monomer of kind α and β is a constant. This parameterization involves 20 parameters, instead of 210 parameters of the MJ matrix, each specifying the strength of a particular residue. Using this parameterization we have found that, for the best fit, all q_{α} are negative and range from -2.3 to 0 , while $\beta = -0.42$. Furthermore, it has been pointed out that the origin of the additive term is due to the hydrophobic effect, while the second order term is responsible for the segregation of dissimilar residues.

Using this parameterization, we can write the Hamiltonian of the chain in a form [10]

$$H = \vec{q}\vec{n} + \frac{\beta}{2}\vec{q}C\vec{q}, \quad (3)$$

where \vec{n} and \vec{q} have dimensions equal to the number of monomers in the chain. The i -th coordinate of \vec{n} is the number of nearest neighbors for the i -th monomer and the i -th coordinate of \vec{q} specifies the strength of the residue in the i -th site. C is the contact matrix for a given conformation. In the above reference it has been shown that the Hamiltonian (3) fits very well the original MJ Hamiltonian and, what is more precious, it is very convenient to handle analytically.

One of the problems that can be solved easily using the above Hamiltonian is, given a target structure (C matrix and \vec{n}) and the composition of the chain in term of residues, to

find the sequence which minimize the energy [10]. Particularly, using the fact that the second order term is usually 2–3 times smaller than the first order term, a first order approximation solution can be found minimizing only the solvent exclusion term. The straightforward way is to choose a sequence so that the vectors \vec{q} and \vec{n} are as anti-parallel as possible, keeping the constraint of a fixed number of different kinds of monomers. Knowing that all components of \vec{q} are negative while all components of \vec{n} are positive, it is necessary to put the residues with the most negative value of q_i in the sites of the target structure with the largest number of nearest-neighbors. The effect is, roughly speaking, to put 'hydrophobic' residues (i.e. low q_i) inside the structure while keeping 'hydrophilic' ones (high q_i) on the surface. The second order term in the Hamiltonian (3) is responsible for a fine tuning of residue distribution, mostly inside the hydrophobic/hydrophilic regions, and causes a further decrease of the sequence energy.

III. MUTATIONS AND HOT SITES

According to [1], we label each mutation with the difference of the native state energy of the wild-type sequence and of the mutated sequence

$$\Delta E_{loc} = \frac{1}{2} \sum_{ij} (B_{ij}^0 - B_{ij}^\alpha) \Delta(r_i - r_j), \quad (4)$$

where B_{ij}^0 is the interaction element associated with the wild-type sequence and B_{ij}^α with a mutated sequence. It has been shown that the information about the thermodynamic features of the mutated sequence is mostly contained in the value of ΔE_{loc} [6], [11].

The energetic effects of mutations in a given site i are studied introducing the average ΔE_{loc} over the 19 possible mutations in this site,

$$\overline{\Delta E_{loc}}(i) = \frac{1}{19} \sum_{\alpha} \sum_j (B_{ij}^0 - B_{ij}^\alpha) \Delta(r_i - r_j). \quad (5)$$

For optimized sequences there are few sites (up to 10%) where $\overline{\Delta E_{loc}}$ is large ($\sim \Delta$, where Δ is the gap between the native state and the random conformations energy [2]), while for

the others $\overline{\Delta E_{loc}}$ is much lower. We call the former sites 'hot' and the latter 'cold'. If a mutation occurs in a 'hot' site, there is a high probability that it fills the gap, eliminating the feature of design and causing misfolding of the chain.

For random interaction matrices whose elements have Gaussian distribution, the behavior of hot sites is the same as indicated in Ref. [1]. Hot sites can be both in the bulk and on the surface of the native configuration (See Fig. 1b) with dominance of 'hot' sites in the bulk.

On the other hand, in a model with only two kinds of residues (H and P), the optimization of the sequence puts H residues in the sites with the highest number of nearest neighbors. In this case (see Ref. [7]), every site containing a H residue is a hot site.

We are now interested in studying the pattern of hot sites in a model where the interaction matrix contains both features of hydrophobic-hydrophilic separation and randomness or complicated non-linearity.

IV. CONSTRUCTION OF THE MAP OF 'HOT' AND 'COLD' SITES

To investigate the behavior of $\overline{\Delta E_{loc}}(i)$ we use the parameterized Hamiltonian (3). It is straightforward to show that, for a wild-type sequence characterized by \vec{q}

$$\overline{\Delta E_{loc}}(i) = -(n_i + \beta \sum_j^L C_{ij} q_j)(q_i - \langle q \rangle_\alpha), \quad (6)$$

where $\langle q \rangle_\alpha = 1/20 \sum_{\alpha=1}^{20} q_\alpha$, is the average of the values q_α corresponding to the 20 monomers different from the wild-type. With this assumption we have found $\langle q \rangle_\alpha \approx -1.23$.

We shall consider first the case $\beta = 0$, which is exactly solvable, and then the consequences of the non-linear term introduced via non-zero 'mixing' parameter β .

A. $\beta = 0$

In the case $\beta = 0$ the Hamiltonian contains only the solvent exclusion term $H_0 = \sum_i q_i n_i$. As we discussed earlier, optimization of the sequence, given a structure, consists in putting

the most hydrophobic residues into the sites with the greatest number of contacts, keeping with the constraint of fixed number of different residues, so that

$$q_i \approx \frac{\sum_{i=1}^L q_i}{\sum_{i=1}^L n_i} n_i. \quad (7)$$

For short chains and 20 letter code used in the model with $\beta = 0$ the optimization procedure described above works reasonably good in constructing optimal sequences while for longer chains it seems that the model is not adequate to ensure a single ground state or a ground state well-separated from the other states. Nevertheless, the case $\beta = 0$ is a good starting point to investigate the role of the different terms of Hamiltonian (3).

In this case equation (6) can be written as

$$\overline{\Delta E_{loc}}(i) = -n_i(q_i - \langle q \rangle_\alpha). \quad (8)$$

Defining $\langle q \rangle = \sum_{i=1}^L q_i / \sum_{i=1}^L n_i$ and substituting (7) in (8) as an approximation for an optimal sequence, we obtain

$$\overline{\Delta E_{loc}}(i) = -n_i \langle q \rangle (n_i - \frac{\langle q \rangle_\alpha}{\langle q \rangle}). \quad (9)$$

For typical values of $\langle q \rangle \sim -0.6$ and $\langle q \rangle_\alpha \sim -1.26$ then

$$\overline{\Delta E_{loc}}(i) \approx 0.6n_i(n_i - 2.1). \quad (10)$$

The shape of this function is plotted in Fig. 2. It is interesting to compare the value $\overline{\Delta E_{loc}}(i)$ for the optimized sequence with the one for a random sequence. We will identify, in the spirit of Random Energy Model [12], 'hot' sites (as defined in Sect. III) with those sites in which the average impact of mutations is greater than for a random sequence. We define a sequence to be random if there is no correlation between the strength q_i at a given site, and its number of nearest neighbors n_i , so that

$$\overline{\Delta E_{loc}^{rand}}(i) = -n_i(q - \langle q \rangle_\alpha), \quad (11)$$

where q ranges between -2.3 and 0 . The values that $\overline{\Delta E_{loc}^{rand}}(i)$ can assume are comprised between the two straight lines plotted in Fig.2a. While the dependence of $\overline{\Delta E_{loc}}(i)$ for the

random sequence is linear, for a selected sequence it is quadratic. In the case of the selected sequence the quadratic behavior of the mutation energy versus the number of closest nearest neighbors induces a sharp distinction between bulk sites ($n \gtrsim 3$) and surface sites. As clear from (Fig. 2a), all bulk sites are 'hot', while surface sites are 'cold'. As consequence, 'hot' sites have a certain degree of symmetry in target structures, i.e. no one of the sites with the same number of nearest neighbors is privileged to the others. The map of the 'hot' and 'cold' sites for a Hamiltonian $\beta = 0$ and a 36 monomer target structure is presented on (Fig. 1c).

B. $\beta \neq 0$

If β is not zero, but still small in absolute values, it is possible to minimize the energy of the sequence in two steps, first minimizing $H_{\beta=0} = \vec{n}\vec{q}$ and finding an initial trial optimal sequence \vec{q}_{tr} , and then re-minimizing the same $H_{\beta=0}$ with an effective $\vec{n}_{eff} = \vec{n} + \frac{\beta}{2}\vec{q}_{tr}C$. As was shown in Ref. [10] this procedure is quite reliable for small β .

Using the same approximation (7) as in the previous section for \vec{q}_{tr} one finds

$$\overline{\Delta E_{loc}^{\beta}}(i) \approx -n_i \langle q \rangle (1 + \beta \langle q \rangle \frac{N_i}{n_i}) (n_i - \frac{\langle q \rangle_{\alpha}}{\langle q \rangle}) \quad (12)$$

where $N_i = \sum_j C_{ij}n_j$ is the number of nearest neighbors of the nearest neighbors of site i and can assume values in the range $\{n_i, \dots, 4n_i + 1\}$. The expression of $\overline{\Delta E_{loc}^{\beta}}(i)$, then, takes into account, through the value of N_i , sites lying further than the nearest neighbors of i . As consequence of this, we can observe (Fig. 2b) a broadening of the range of values that $\overline{\Delta E_{loc}^{\beta}}(i)$ can assume for each n_i (we will refer to this broadening as 'energy bands' in our further discussion)

From Fig. (2b) it follows that the effect of the segregation term in (3) is to differentiate among the sites with the same number of closest nearest neighbors. As $\beta \neq 0$, the second shell of nearest neighbors starts playing its role, thus introducing a cooperative effects in the determination of $\overline{\Delta E_{loc}^{\beta}}(i)$. This splitting of the degeneracies in the $\overline{\Delta E_{loc}^{\beta}}(i)$ at $\beta \neq 0$ can

lead to the overlap of 'energy bands' thus leading to the possibility of encountering a 'hot' site on a surface and 'cold' site in the bulk.

To summarize, from the point of view of single mutations, in the case $\beta = 0$ the spectrum of mutations is composed by two main parts, namely mutations in bulk sites, with high value of ΔE_{loc} , and mutations in surface sites, with ΔE_{loc} close to zero or negative. The effect of the coupling term is to broaden the range of the possible mutation energies for the mutation sites of the same type (bulk or surface) mixing the energetic levels corresponding to mutations in different kind of sites. So, the symmetry of hot sites in the target structure can be broken thus allowing some hot sites to be found on surface.

C. Explicit Calculations with MJ parameterized Hamiltonian

To investigate how the 'energy bands' depend upon the strength of the nonlinear contribution in the interaction matrix we have made some explicit calculations, using as target structure the 36mers chain displayed on (Fig. 1). We have first calculated the best values of q_α and β to fit MJ matrix according to Eq. 2, finding $\beta = -0.42$. Using these values for q_α , we varied β in the range $(-1.5, 1.5)$, optimizing each time the sequence with a genetic energy minimization technique. The composition has been kept fixed for all values of β and chosen in such a way as to satisfy $q_i \sim n_i$ (condition for optimal composition at $\beta = 0$). For the sake of computational convenience, the interaction matrix elements have been rescaled to have zero average and standard deviation equal to 1.0. Then, we have plotted the value of $\overline{\Delta E_{loc}^\beta(i)}$ for each lattice site, as function of β . First, we consider the case $\beta < 0$. The raising of different 'energy bands' is shown in Fig.3a. For $-0.7 \lesssim \beta < 0$ all the bands lay into four distinct groups. The first two groups, which correspond to the sites with $n_i = 1$ or $n_i = 2$, contribute to cold sites. The other two groups correspond to the sites with $n_i = 3$ or $n_i = 4$ defining the 'warm' and 'hot' sites. This situation is very similar to the case of $\beta = 0$, where bands do not overlap and 'hot' sites are exclusively in the bulk. It is not surprising to find the same distribution pattern for the MJ matrix ($\beta = -0.42$) (Fig.1d).

and HP-like interaction matrix ($\beta = 0$) (Fig.1c). For $-2.5 \lesssim \beta \lesssim -1.0$ the nonlinear part of the interaction matrix starts playing its role. As was shown in the previous section the second neighbor shell contribute to the value of $\Delta E_{loc}^\beta(i)$. At these values of parameter β we observe that some of the energy bands corresponding to 'warm' (n=3) and 'cold' sites (n=1,2) mix, while the bands corresponding to the 'hot' sites stay well separated from the other bands.

In the case of $\beta > 0$ (Fig.3b) the non-linear effect is much more dramatic. For $\beta \gtrsim 0.2$ all bands start mixing allowing 'cold' sites penetrate the bulk while pushing 'hot' sites on a surface. We can rationalise the different pattern of 'energy bands' at $\beta < 0$ and $\beta > 0$ by examining the Eq.6 and Hamiltonian 3. Noticing that $\frac{\beta}{2}\vec{q}C\vec{q}$ is of the order of $\frac{\beta}{2}\vec{q}\vec{n} < q >$ we can rewrite the Hamiltonian 3 in a form

$$H = \vec{q}\vec{n}(1 + \frac{\beta}{2} < q >) + \beta\eta \quad (13)$$

where η contains the collective effects and $\vec{q}\vec{n}(1 + \frac{\beta}{2} < q >)$ describes a 'renormalized' hydrophobic effect. In the case $\beta < 0$, $(\frac{\beta}{2} < q >) > 0$ and the interaction matrix is largely dominated by the hydrophobic effect, while the collective contribution to the Hamiltonian is not strong enough to substantially mix the 'energy bands'.

For the $\beta > 0$ case $(\frac{\beta}{2} < q >) < 0$ and the renormalized hydrophobic effect becomes comparable or smaller than the collective term in the Hamiltonian. This allows all bands to mix substantially.

D. Explicit Calculations for Random Hamiltonian

Another interesting question which can be addressed is how our conclusions are modified by the addition of a random term in the $\beta = 0$ Hamiltonian. To study this problem, we have chosen a Hamiltonian in the form

$$H = \vec{n}\vec{q} + \gamma \frac{1}{2} \sum_{ij}^L \epsilon_{ij} \Delta(r_i - r_j), \quad (14)$$

where \vec{nq} comes from the parameterization (2) of the MJ matrix with $\beta = 0$. The virtue of this Hamiltonian is in separation in a controllable manner the hydrophobic effect due to the \vec{nq} and any other non-linear effects are modeled by the random term. The values of ϵ_{ij} are taken from a Gaussian distribution with mean zero and standard deviation 1.0. In (Fig. 4) the 'energy bands' are shown as a function of 'mixing' parameter γ . The overall pattern is exactly the same as discussed in the previous section for the case in which non-linear terms in the parameterization are switched on leading to the effect of 'band crossing' thus allowing 'warm' sites to appear on the surface and 'cold sites' in the bulk. Even in the case of 'band crossing', there is still a clear trend for the 'hot' and 'warm' sites to concentrate in the bulk of the structure. This is due to the fact that bulk sites, building the biggest number of contacts, still display the strongest response to point mutations.

In the inserts of Figs.3a,b and Fig.4 shown the energy of the optimal non-mutated sequence for different values of β and γ , respectively. It is possible to observe a sudden decrease in energy of the optimal sequence as β and γ increases signifying that the addition of non-linear terms into a Hamiltonian allows for a much better energy minimization.

V. CONCLUSIONS

In this work we have considered how the regularity of the interaction matrix influence the distribution pattern of 'hot' sites. It has been found that if the matrix is polarized (dominant hydrophobic effect, $\beta \sim 0$ or $\gamma \sim 0$) this distribution is very simple. All the 'hot' sites can be found at the positions with maximum number of closest nearest neighbors (bulk).

With increasing importance of non-linear terms ($\beta \neq 0, \gamma \neq 0$) the distribution pattern changes so that the 'hot' and 'warm' sites can be found in places with smaller number of nearest neighbors (surface) while the general trend of the 'hot' sites to fall into a bulk part of a conformation still holds.

As pointed out above this can be rationalized by noticing that if mixing parameter is

different than zero each site starts feeling not only its nearest neighbors but also the more distant sites. This leads to a collective nature of the interactions giving rise to a modified distribution pattern of 'hot' sites.

REFERENCES

- [1] G. Tiana *et al.*, J. Chem. Phys. **108**, 757 (1998)
- [2] E. Shakhnovich, Phys. Rev. Lett. **72**, 3907 (1994)
- [3] E. Shakhnovich, A. Gutin, Protein Eng. **6**, 793 (1993)
- [4] T. E. Creighton, *Proteins*, W. H. Freeman and Co., New York, 1993
- [5] Table V in S. Miyazawa and R.L. Jernigan, Macromolecules **18**, 534 (1985)
- [6] R. A. Broglia, G. Tiana *et. al.*, to be published
- [7] H. Li, R. Helling, C. Tang, N. Wingreen, Science **273**, 666 (1996)
- [8] Table III in S. Miyazawa and R.L. Jernigan, Macromolecules **18**, 534 (1985)
- [9] H. Li, C. Tang, N. Wingreen, Phys. Rev. Lett. **79**, 765 (1997)
- [10] M. Skorobogatiy, H. Guo, M. Zuckermann, Macromolecules, **30**, 3403 (1997)
- [11] H.J. Bussemaker, D. Thirumalai, and J.K. Bhattacharjee, Phys. Rev. Lett. **79**, 3530 (1997)
- [12] B. Derrida, Phys. Rev. B **24**, 2613 (1981)
- [13] V. Abkevich, A. Gutin, E. Shakhnovich, J. Chem. Phys **101**, 6052 (1994)

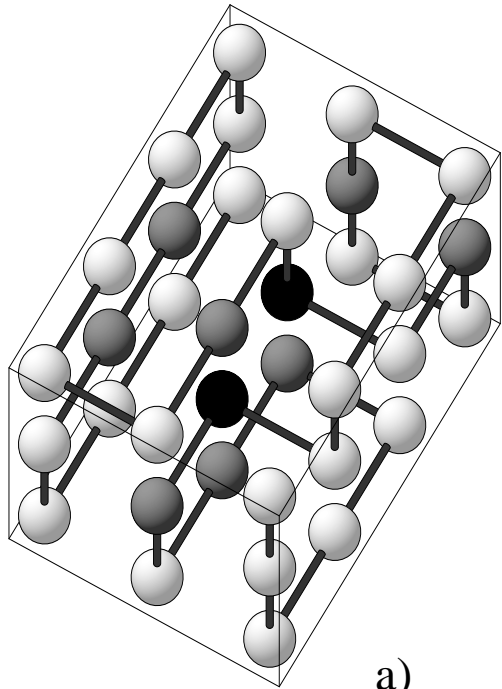
FIGURES

FIG. 1. a) Map of the 'hot' (black), 'warm' (dashed) and 'cold' (white) sites for the random Gaussian matrix. b) Map of the mutation sites for the randomly generated Gaussian matrix. c) Map of the mutation sites for the LTW parameterization of MJ matrix with $\beta = 0$. d) Map of the mutation sites for the MJ interaction matrix (HP like model).

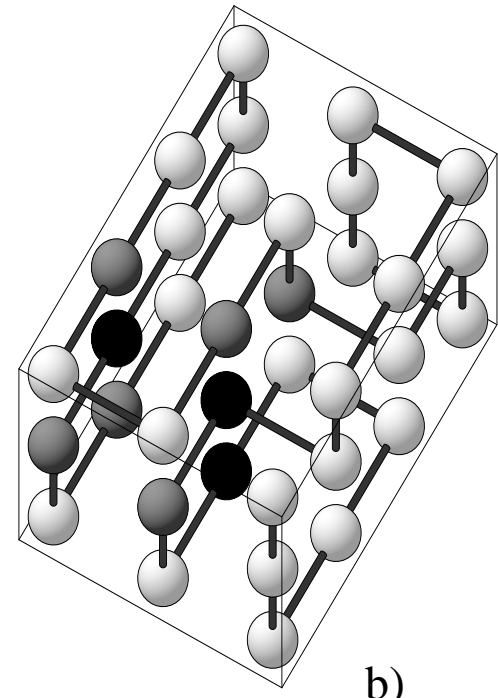
FIG. 2. a) Energy of mutation as a function of the number of closest nearest neighbors for LTW parameterized interaction matrix with $\beta = 0$. ΔE_{loc} for the optimized sequence exhibits nonlinear behavior leading to the sharp differentiation of 'hot' and 'cold' sites. While ΔE_{loc} for the random sequence can have both positive and negative values at any n leading to the possibility of finding a 'hot' mutation even at $n = 1$. b) Energy of mutation as a function of the number of closest nearest neighbors for LTW parameterized interaction matrix with $\beta < 0$. As second nearest neighbors start contributing to the mutation energy the energy line broadens thus allowing for the sites with equal number of closest nearest neighbors to have different interaction energies. All possible ΔE_{loc} are confined between the two parabolas shown on a graph.

FIG. 3. Energy bands for 36 mutation sites. The interaction energy matrix is based on LTW parameterization with β parameter introducing a non-linear segregation energy in Hamiltonian. Different line types correspond to the sites with different number of closest nearest neighbors. So, for example, solid lines correspond to the mutation energy of the sites 16 and 27 that have the most number of closest nearest neighbors. Sites with 4,3,2 and 1 closest nearest neighbors are specified by solid, dashed, solid-dashed and dotted lines respectively. a) corresponds to $\beta < 0$ b) corresponds to $\beta > 0$. In the insert the energy of the optimal non-mutated sequence is shown for different values of β .

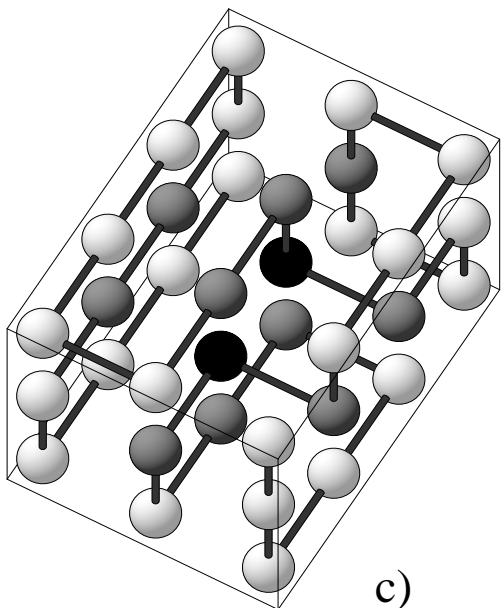
FIG. 4. Energy bands for 36 mutation sites. The interaction energy matrix is a mix of LTW parameterized matrix with $\beta = 0$ and Gaussian random matrix. The mixing with random matrix is controlled by the parameter γ . At $\gamma = 0$ the interaction matrix is pure LTW with $\beta = 0$ while at $\gamma \sim 2.0$ the elements of random matrix become comparable to the elements of the regular matrix. Different line types correspond to the sites with different number of closest nearest neighbors. So, for example, solid lines correspond to the mutation energy of the sites 16 and 27 that have the most number of closest nearest neighbors. Sites with 4,3,2 and 1 closest nearest neighbors are specified by solid, dashed, solid-dashed and dotted lines respectively. In the insert the energy of the optimal non-mutated sequence is shown for different values of γ .



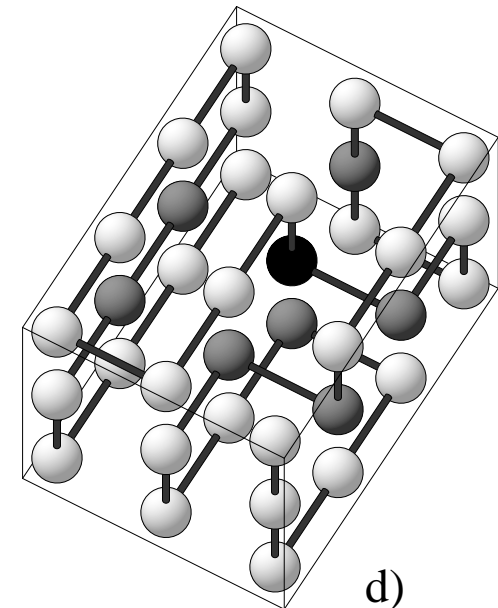
a)



b)

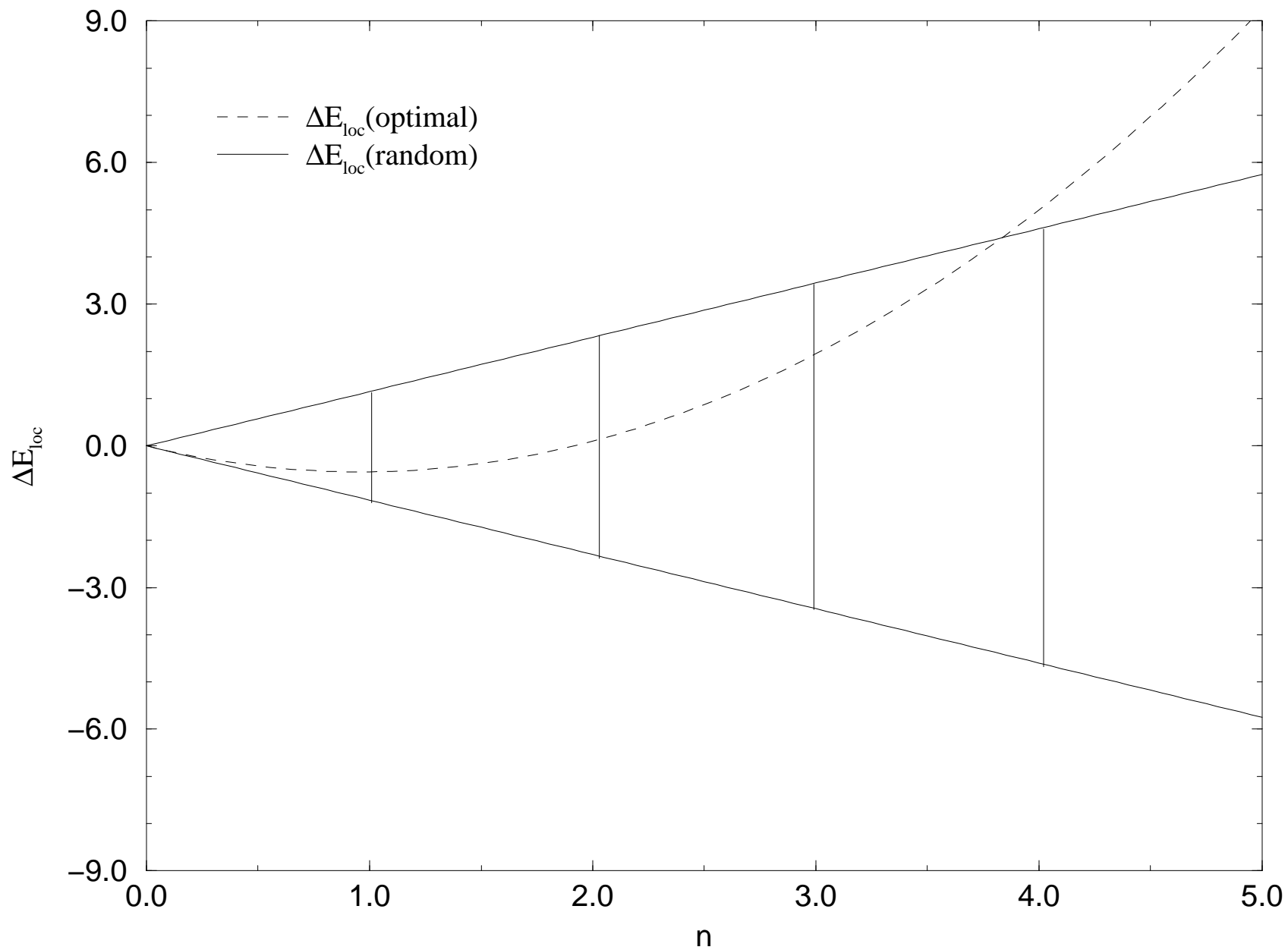


c)

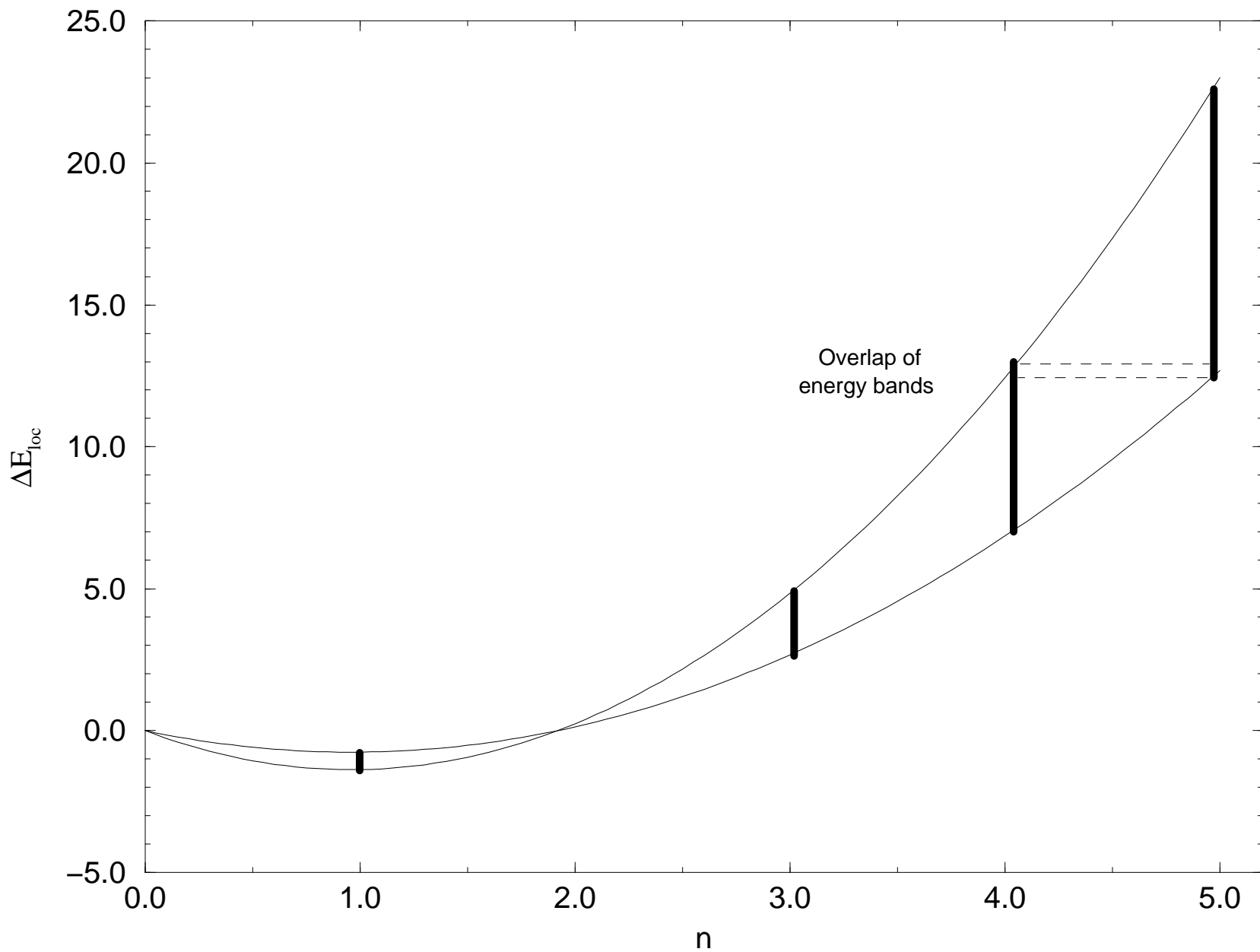


d)

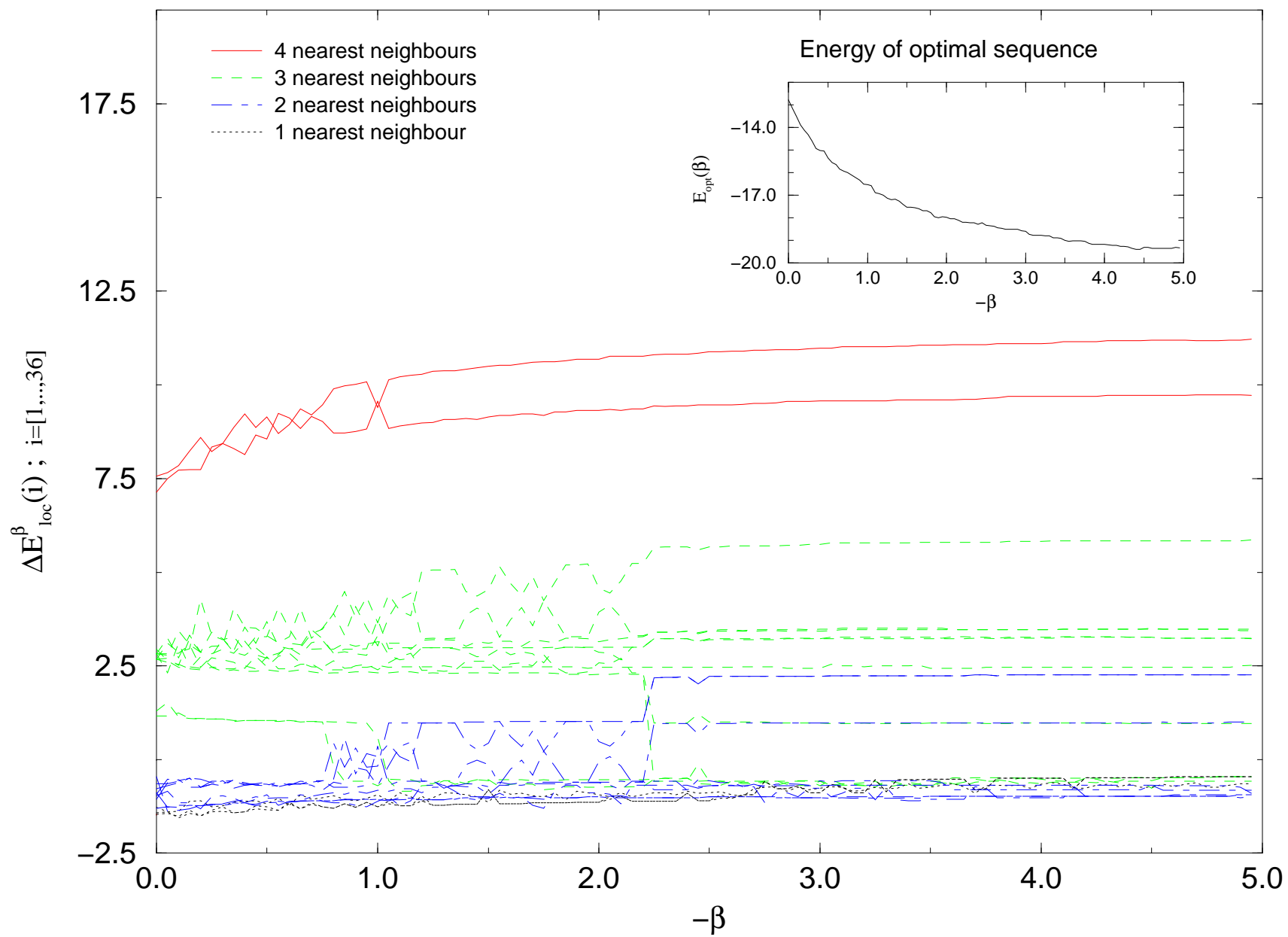
Energy of mutation for $\beta=0$ LTW parametrization



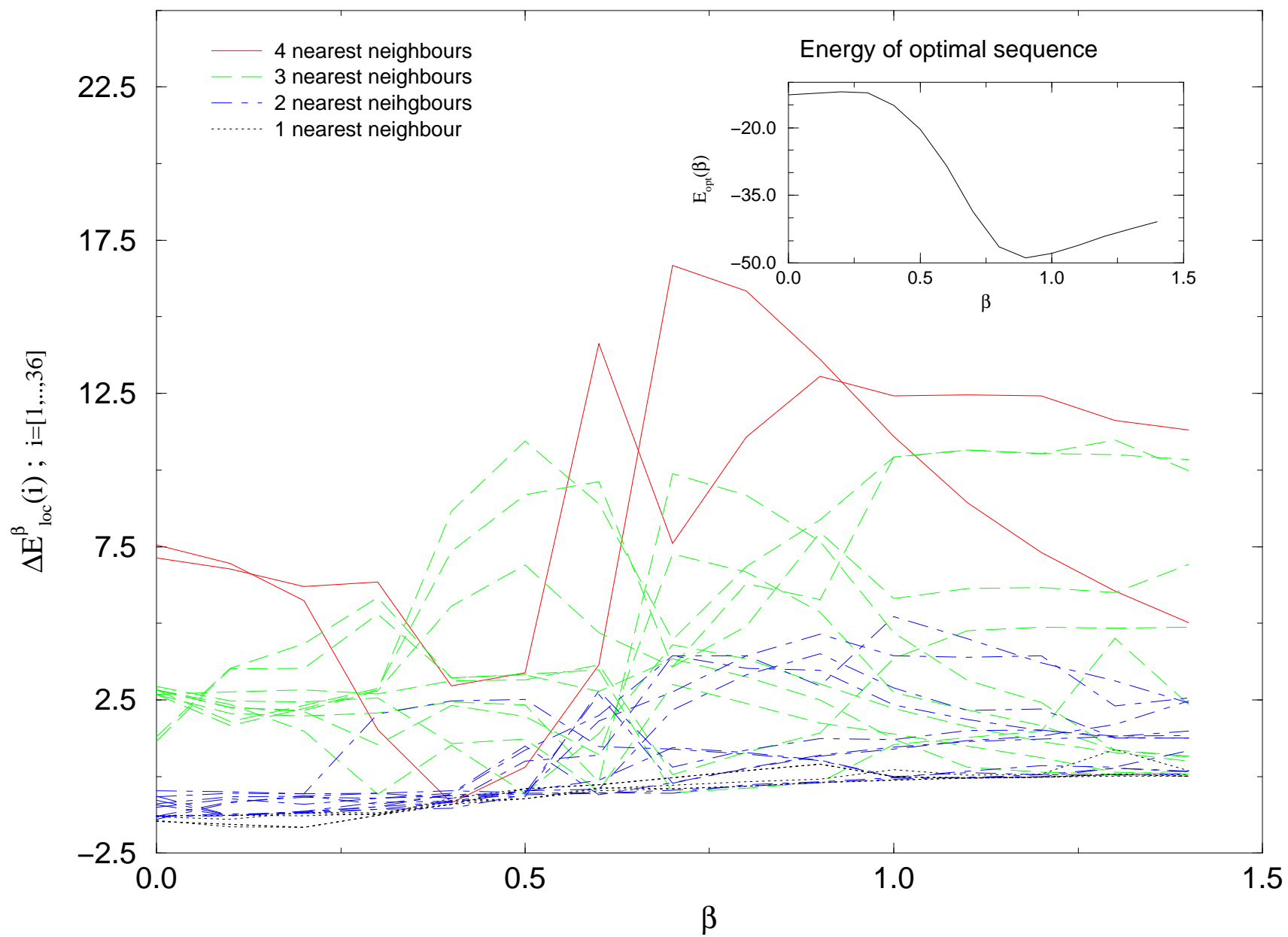
Energy of mutation for $\beta=-0.42$ LTW parametrization



Energy Bands for 36 Mutation Sites



Energy Bands for 36 Mutation Sites



Energy Bands for 36 Mutation Sites

